ARTICLES
https://doi.org/10.1038/s41561-018-0094-8
nature geoscience

Efficient cooling of rocky planets by intrusive magmatism

Diogo L. Lourenço[1,2*], Antoine B. Rozel[1], Taras Gerya[1] and Paul J. Tackley[1]

The Earth is in a plate tectonics regime with high surface heat flow concentrated at constructive plate boundaries. Other terrestrial bodies that lack plate tectonics are thought to lose their internal heat by conduction through their lids and volcanism: hotter planets (Io and Venus) show widespread volcanism whereas colder ones (modern Mars and Mercury) are less volcanically active. However, studies of terrestrial magmatic processes show that less than 20% of melt volcanically erupts, with most melt intruding into the crust. Signatures of large magmatic intrusions are also found on other planets. Yet, the influence of intrusive magmatism on planetary cooling remains unclear. Here we use numerical magmatic-thermo-mechanical models to simulate global mantle convection in a planetary interior. In our simulations, warm intrusive magmatism acts to thin the lithosphere, leading to sustained recycling of overlying crustal material and cooling of the mantle. In contrast, volcanic eruptions lead to a thick lithosphere that insulates the upper mantle and prevents efficient cooling. We find that heat loss due to intrusive magmatism can be particularly efficient compared to volcanic eruptions if the partitioning of heat-producing radioactive elements into the melt phase is weak. We conclude that the mode of magmatism experienced by rocky bodies determines the thermal and compositional evolution of their interior.

A diverse range of tectonic regimes can be observed on the surface of terrestrial planets and moons across the Solar System. These different tectonic behaviours are the surface expression of their interior dynamics, which are mainly driven by cooling from the top and different interior heat sources. These include primordial heat left from the accretion and differentiation of the body, radioactive decay of heat-producing elements (HPEs) and tidal heating[1]. Surface tectonics and magmatism control the transport of heat from the interior to the surface[2]. Many terrestrial bodies, such as Mercury, Mars and the Moon, show little or no evidence of surface motion, probably because they are covered by a thick and non-yielding lithosphere (the stiff topmost layer of rocky bodies). In these cases, heat is mostly lost by conduction across the thick lid in an inefficient way, leading to low heat flows[3,4]. Very differently, the Earth is characterized by significant surface motion of lithospheric plates that are continuously formed, cooled and recycled back into the mantle. This regime is known as plate tectonics and is characterized by high average surface heat flow, predominantly concentrated along constructive plate boundaries where plates form, which leads to efficient planetary cooling[2]. There is, however, an example of a terrestrial body with a higher surface heat flow than the Earth but without the presence of plate tectonics: Jupiter's moon Io[5], which is heated mainly by tidal interactions with Jupiter[6]. Heat is lost from its interior through volcanic channels that cut the lithosphere and transport material and heat to the surface. This volcanic-eruption-driven regime is known as the heat-pipe mode, and it is thought to be one of the most efficient modes of cooling internally convecting rocky planets and moons[7–9].

Intrusive versus extrusive magmatism

Numerical models of global mantle convection have been employed for some decades to study tectonic regimes active on Earth and other terrestrial bodies (for a review, see the introduction of ref. [10]). These thermal convection models have brought significant insights into the physical parameters controlling the global tectonic regimes of different celestial bodies, but have usually neglected thermal and/or compositional effects related to mantle-derived magmatism and crust production. Only over the last decade have numerical models started to systematically take into account magmatic processes, which have a critical role in differentiating the mantle. These processes happen when the temperature of a rock exceeds the solidus temperature, and consequently partial melt is generated. This generated melt has a different bulk composition from the source rock. In addition, trace elements, some of which produce heat by radioactive decay, are generally incompatible and therefore partition into the melt and are transported together with it[11]. When melt crystallizes at the planetary surface, the newly formed rock is strongly radioactive, which affects the dynamics of the lithosphere and enhances surface heat loss[12–15]. This geochemical effect is missing in simplified thermal convection models, but it may play a critical role for the planetary cooling and evolution. Thermo-magmatic mantle convection models allow self-consistent modelling of HPEs transport. Furthermore, in recent years, this new type of model has helped in the understanding of some features of plate tectonics[13,16,17], and potentially early Earth[9] and Venus[18]. However, they still employed a simplified approach, by assuming that magmatism is completely extrusive (volcanic) (that is, the heat-pipe mode). Yet, field studies on Earth observe that volumes of intruded magmas are 4–9 times larger than those of erupted magmas[19,20]. On Venus, there is also extensive evidence of crustal plutonism (that is, intrusive magmatism) possibly fed by mantle plumes[21], in the form of hundreds of corona and 64 nova structures[22–24]. Thus, intrusive magmatism could potentially play a greater role than volcanism in the dynamics of the lithosphere and the mantle of rocky planets and moons, and must be taken into account when modelling their long-term evolution and cooling histories.

Motivated by these observations, recent modelling studies have focused on the effects of intrusive magmatism by varying the eruption efficiency in global models of thermo-magmatic mantle convection[25]. The results showed that plutonism could indeed play a

[1]Institute of Geophysics, Department of Earth Sciences, ETH Zurich, Zurich, Switzerland. [2]Present address: Department of Earth and Planetary Sciences, University of California, Davis, CA, USA. *e-mail: dlourenco@ucdavis.edu

crucial role in the dynamics of the lithosphere by warming and softening the planetary lid and thereby triggering lithospheric dripping and delamination. Furthermore, intrusive magmatism creates localized lithospheric-scale weak zones that separate strong plates. This recently discovered tectonic regime, named the plutonic squishy lid regime, can explain the formation of primordial tonalite–trondhjemite–granodiorite continental crust on early Earth[25].

In this study, we focus on the influence of intrusive magmatism on planetary cooling. We investigate the effects of eruption versus intrusion efficiency and partitioning of HPEs into the melt phase on lithospheric dynamics, surface heat flux and the overall state of the mantle, in a rocky body that does not experience subduction in its entire history. We compare the results to those of previous studies considering 100% eruption efficiency (that is, heat-pipe) and no partitioning of HPEs[9,17] and demonstrate that the effects of magmatism are even more dramatic and paradoxical than previously thought.

We perform numerical simulations of thermo-magmatic mantle convection with spontaneously growing basaltic crust using the code StagYY[26], which allows variable eruption efficiency and radioactive element partitioning. Furthermore, StagYY takes into account phase transformations (including eclogite formation) in the crust and mantle, as well as mantle buoyancy caused by depletion induced by the removal of basaltic melt. All simulations incorporate realistic rheological and physical parameter values[17], and span 4.5 Gyr of core and mantle evolution in a two-dimensional spherical annulus geometry[27]. A large lithospheric yield stress (300 MPa) is imposed to avoid yielding and plate tectonics, making the model appropriate for most convecting bodies of the Solar System (in particular Venus and Io). We investigate the impact of several parameters. First, we investigate convective vigour, changed by systematically testing different reference viscosities (see Methods): 10^{20}, 3×10^{20} and 10^{21} Pa s. These values are consistent with previously published viscosity depth profiles resulting from joint inversion of the geoid and postglacial rebound data[28,29]. Second, we investigate eruption versus intrusion efficiencies. In our simulations, melt generated above the depth of neutral buoyancy (prescribed as ~300 km for models simulating the Earth) is partly extruded to the surface, where it forms basaltic crust with the surface temperature, while the rest is intruded warm at the base of the crust (see Methods). Thus, all of the transported melt is either extruded or intruded, and none is left behind. In this study, eruption efficiencies of 0, 10, 20, 30, 50, 70, 90 and 100% are tested. These values are predefined and are kept constant for each simulation. In nature, extrusion efficiencies are likely to evolve with time because they are the result of migration processes that depend on the structure of the lithosphere and crust. One alternative for dealing with magma migration in a more realistic way would be solving permeable flow in the solid mantle by employing two-phase flow physics[30–35]. However, this approach requires computationally expensive calculations that cannot simulate long geological timescales, on the order of billions of years, as needed in this study to investigate planetary evolution. Therefore, employing fixed values for extrusion efficiency is a convenient simplification, which allows for the exploration of a wide-ranging number of scenarios. Third, we investigate partitioning of HPEs between solid and melt, which is given here by $D_{\mathrm{part}} = C_{\mathrm{solid}}/C_{\mathrm{melt}}$, where C is the concentration of the element in question. In the present work, we consider four different values for D_{part}: 1, 0.3, 0.1 and 0.01. Trace elements that have heat-producing isotopes, such as thorium, uranium and potassium, tend to enter the melt phase, which means that lower values for D_{part} are in better agreement with observations[11]. For clarity of reading, we should mention that, by definition, a lower D_{part} implies a stronger partitioning of HPEs. The partition of HPEs is expected to affect planetary heat losses[36,37].

Effects of eruption efficiency

Figure 1 shows the remarkable effects of different eruption efficiencies, partitioning of HPEs and reference viscosities on the upper-mantle temperature (averaged over a 200 km window below the lithosphere), the average crust thickness, the harzburgitic enrichment at 1,500 km depth and the basal layer thickness above the core–mantle boundary (CMB). These quantities are averaged over the last 500 Myr of the evolution of the planet, that is, from 4 to 4.5 Gyr (present-day). Figure 1a–c demonstrates that high eruption efficiencies and weak partitioning of HPEs lead to higher internal temperatures, and are therefore less efficient at cooling the mantle. The fact that high eruption efficiencies are not more efficient at cooling the mantle is a surprising result, as heat-pipe volcanism instantaneously (on geological timescales and in our simulations) cools down erupted magmas to the surface temperature. This effect is less pronounced for strong partitioning of HPEs and lower reference viscosities. Figure 1d–f shows that the crust thickness increases with increasing eruption efficiency. In the heat-pipe regime, simulations without partitioning of HPEs can grow a crust as thick as 250 km. The same simulations have the highest internal temperatures, as can be seen in Fig. 1a–c. Indeed, a very thick lithosphere insulates the upper mantle from the surface, preventing efficient cooling, even in the heat-pipe mode. Lower D_{part} values lead to stronger partitioning of HPEs into the crust, which results in a warmer crust and therefore thinner crustal thicknesses (Fig. 1d–f). Finally, lower reference viscosities limit crustal thicknesses by convective erosion of the bottom of the lithosphere[2]. Even in such cases, high intrusion efficiencies have a dominant role by further thinning the crust.

Figure 1g–i depicts the state of internal depletion (absence of basaltic material) at mid-mantle depths. In general, high eruption efficiencies and weak partitioning of HPEs strongly deplete the mantle. The causes for this are that heat-pipes form both a thick crust where basalt/eclogite is stored, and a cold lithosphere that prevents crustal recycling. As previously mentioned, HPEs partitioning into the melt (and therefore into the formed basaltic crust) decreases the thickness of the crust by making its erosion easier, which results in a higher enrichment of eclogite in the mantle. Finally, Fig. 1j–l shows the thickness of the basal layer above the CMB. This layer is formed by accumulation of basaltic material that drips from the bottom of the crust. Basal layers are thicker for low eruption efficiencies, as plutonism keeps the crust warm and constant drips can form, bringing part of the material to settle at the CMB. Lower reference viscosities also lead to thicker basal layers, as material is reprocessed faster. Therefore, with time, larger volumes of basaltic material settle above the CMB. This process also explains the exception in the trend in Fig. 1g, where the mantle is depleted for low reference viscosity and low eruption efficiencies: so much material settles at the CMB that the mantle gets very depleted as the planet evolves. However, it should be noted that the thickness of the basal layer strongly depends on the basaltic density anomaly in the lowermost mantle, a parameter that remains an upper bound in our study[38].

It seems plausible for a heat-pipe regime to be exceptionally efficient at releasing heat, due to high eruption efficiency transporting heat from the interior directly to the surface. Paradoxically, we show that warm intrusive magmatism can lead to even more efficient mantle cooling. This surprising result is made intelligible in Fig. 2, which illustrates the differences between intrusive and eruptive magmatism on a global scale. The top plot (Fig. 2a) displays the various contributions to the total heat flow (averaged over 4.5 Gyr of evolution) as a function of the eruption efficiency. In the most extreme cases, where partitioning of HPEs is inefficient, fully intrusive magmatism doubles the total surface heat flow compared to fully extrusive (volcanic) magmatism. This result illustrates how strong plutonism can enhance vertical heat conduction through the lithosphere. However, 100% intrusive magmatism might be unrealistic, as some degree of volcanism is generally observed in terrestrial

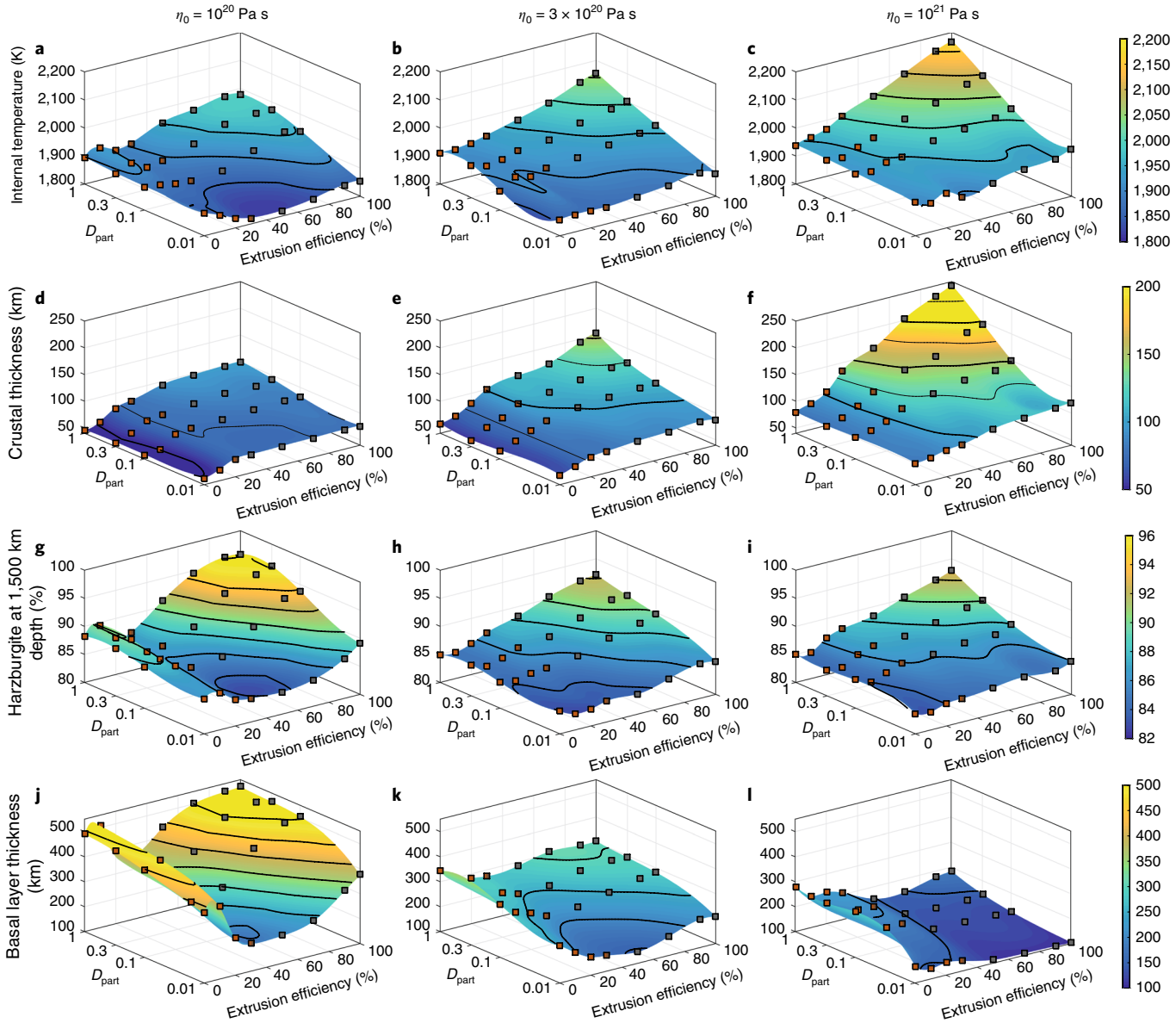

Fig. 1 | Effect of extrusion efficiency and partitioning of HPEs on several averaged quantities over the last 500 Myr of evolution. Each simulation is represented by a square. **a**–**l**, Asthenosphere internal temperature (**a**–**c**), crustal thickness (**d**–**f**), internal depletion represented by the solid harzburgite content at 1,500 km depth (**g**–**i**) and basal basaltic layer thickness around the CMB (**j**–**l**). Results for different reference viscosities are shown: 10^{20} Pa s (**a**,**d**,**g**,**j**), 3×10^{20} Pa s (**b**,**e**,**h**,**k**) and 10^{21} Pa s (**c**,**f**,**i**,**l**).

bodies. A more reasonable situation can be seen around 10 to 30% eruption efficiency[19], where the heat flow increases by 10 TW maximum. This is, nevertheless, a very significant increase of heat flow that has the potential to cool down the mantle by more than 300 K in 4.5 Gyr, in the absence of radioactive heating. The time evolution for various fields of the endmembers shown in Fig. 2a is presented in Supplementary Information.

To understand the paradoxical increase of cooling efficiency of plutonic versus volcanic magmatism, the thermo-compositional structure of the upper mantle needs to be analysed. Figure 2b,c illustrates the thermo-compositional states of intrusive- (Fig. 2b) and eruptive-dominated (Fig. 2c) mantles and the processes that lead to those states. Figure 2b shows that when warm basalt is intruded at the base of the crust, the lithosphere becomes warmer and softer. As a consequence, large basaltic blocks transformed into dense eclogite are delaminated into the mantle. The lithosphere is kept thin, and conductive heat flow is therefore high, which generates cold downwellings. Moreover, the mantle remains enriched in the basaltic component due to constant eclogitic drips and delaminations. This re-fertilizes the depleted upper mantle and thus enhances the potential for further melting without increasing mantle temperature (as the solidus temperature of fertile pyrolitic mantle is lower than that of a depleted harzburgitic one), allowing warm magma to keep being intruded at the base of the crust, even though the planet is cooling very efficiently. This thermo-compositional feedback leads to very effective heat loss. In contrast, Fig. 2c shows a heat-pipe regime where a thick, cold and stable crust is built by eruptive magmatism together with low partitioning of HPEs. Due to little crustal recycling, the upper mantle becomes strongly depleted (that is, harzburgitic in composition) and further melt production requires a significant mantle temperature increase. This explains why the internal temperature rises above the pyrolite solidus, represented by a dashed red curve in the schematic temperature profiles. Since the top boundary layer is very thick, the absence of strong heat

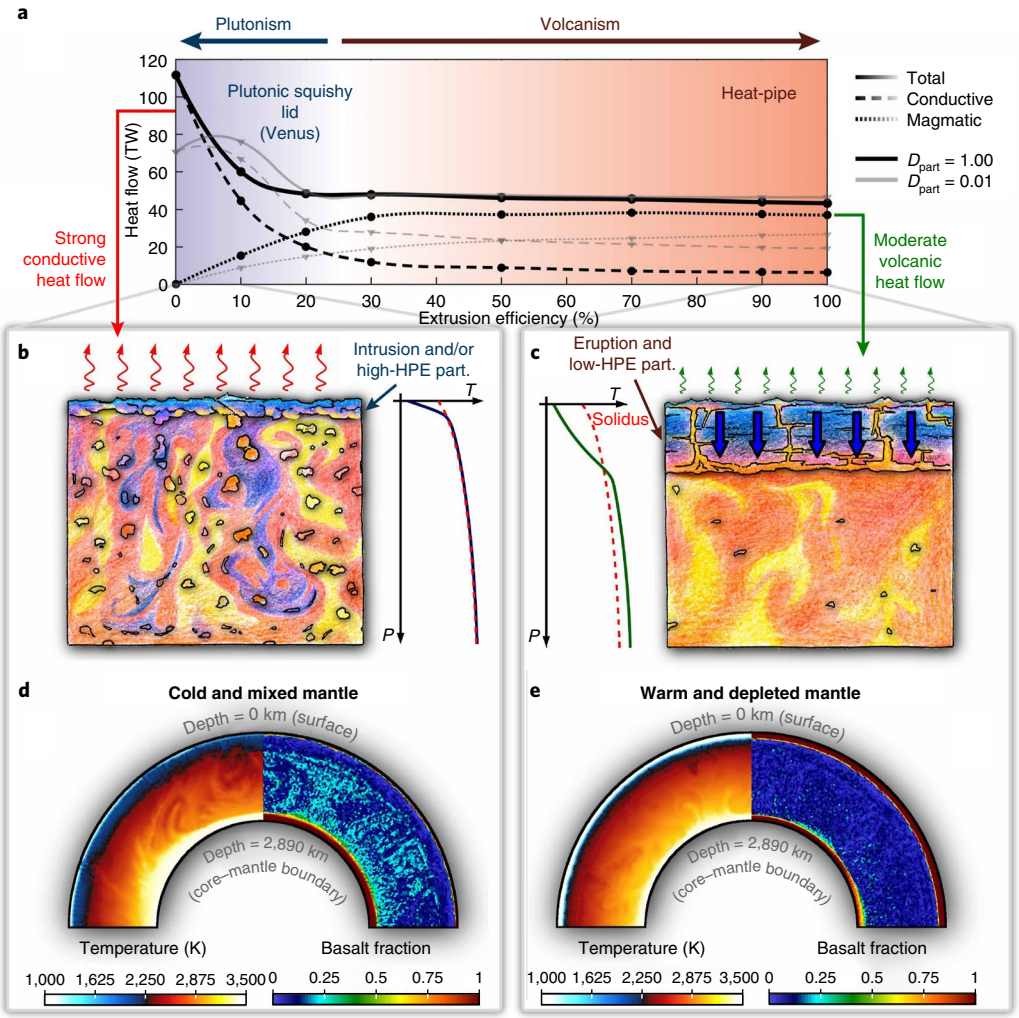

Fig. 2 | Surface heat loss, behaviour and internal state of a planet/moon in a plutonic squishy lid regime versus in a heat-pipe regime. The reference viscosity for these simulations is 10^{21} Pa s. **a**, Conductive, magmatic and total surface heat flow as a function of the eruption efficiency. **b**, Left, an illustration of the dynamics of a plutonic squishy lid. Right, a schematic representation of a typical upper mantle geotherm (solid blue line) and the solidus temperature curve for mixed mantle composition (red dashed line) . Part., partitioning. **c**, Left, an illustration of a typical upper-mantle geotherm (solid green line) and, again, the solidus curve (red dashed line). Right, an illustration of the dynamics of a heat-pipe regime. **d**,**e**, Final temperature and basalt–eclogite distribution at 4.5 Gyr of the evolution of a plutonic squishy lid case with a D_{part} of 1.0 and an extrusion efficiency of 0% (**d**), and of a heat-pipe case with a D_{part} of 1.0 and an extrusion efficiency of 100% (**e**).

conduction prevents vigorous cold downwellings from forming. It is interesting to observe that, in the heat-pipe case, heat is extracted by repeated re-melting and eruption of the base of the crust/lithosphere. The depleted upper mantle slowly warms the crust from below without significant mass exchange between the crust and the mantle. We therefore predict a very limited mantle signature in volcanic magmas in a heat-pipe scenario.

Figure 2d,e depicts the final state of part of the domain of our numerical simulations after 4.5 Gyr of evolution, for the endmember scenario with no partitioning of HPEs. The mantle is much colder in the intrusive case in Fig. 2d (blue upper mantle and apparent dark downwellings) than in the eruptive case in Fig. 2e (black–red upper mantle, few reddish downwellings). The difference in lithospheric thicknesses between the two cases is striking and, when plutonism is considered, the basalt/eclogite component is much more abundant in the entire mantle, which is therefore more fertile.

However, it should be mentioned that, for strong partitioning of HPEs, the endmembers shown in Fig. 2b,c tend to be more similar because HPEs in the crust warm it up and ease its recycling into the mantle. The different regimes possible in a rocky body, depending on the eruption efficiency and D_{part}, are shown in Fig. 3. For low eruption efficiencies, a plutonic squishy lid is expected with dynamics as shown in Fig. 2b. For high eruption efficiencies, two modes are possible, depending on the partitioning of HPEs. If D_{part} is low, the crust is thinner and efficient eruption leads to effective cooling. On the other hand, high D_{part} values lead to a very thick crust (which may reach the depth of neutral buoyancy) and a depleted upper mantle. Since eruption cannot proceed efficiently, melt will accumulate beneath the crust and heat-pipes cannot be maintained. This results in less efficient cooling. We expect that the existence of these different regimes for different planetary bodies depends on their composition and surface conditions. For example, a planet closer to its star or with a very insulating atmosphere (such as Venus) is expected to have a more ductile lithosphere, which leads to higher degrees of intrusion and therefore to a plutonic squishy lid regime. On the other end, a planet far from its star is more likely to have a cold surface, leading to a stiff lithosphere and therefore high eruption efficiencies due to the dominance of vertical magma transport along upward-propagating fractures and dykes in the cold brittle crust[35,39]. Whether the active regime is heat-pipe or thermo-compo-

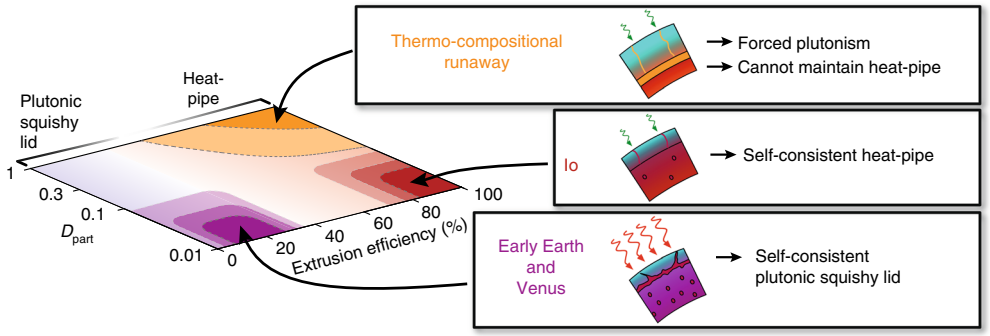

Fig. 3 | Regime diagram of the tectonic regimes discussed in this work. Parameter space in terms of extrusion efficiency and partitioning of HPEs where the different tectonic regimes discussed in this work are expected, together with a brief discussion of them.

sitional runaway will be determined by the partitioning efficiency of HPEs, which can vary from planet to planet depending on temperature, pressure or oxygen fugacity[40]. Io, for example, should experience a heat-pipe regime and not a thermo-compositional runaway because its surface heat flux is high. This distinction is important because, as shown in this work, the final thermal and compositional states of the planet can be very different.

A new paradigm of planet cooling and evolution

The present work shows that the impact of intrusive magmatism on the long-term dynamics of terrestrial planets and moons is much more important than previously expected. Furthermore, the partitioning of heat-producing isotopes can impact the tectonic regime in a rocky body. We demonstrate that the mode of magmatism has to be considered to fully understand the evolution of terrestrial bodies that never experienced long-lasting plate tectonics, and that intrusive magmatism is able to cool the mantle more efficiently than eruptive magmatism. The latter point demonstrates the insulating effect that a heat-pipe regime can have if the crust is not thinned by the presence of HPEs in sufficient concentration. These results have severe implications for the study of the evolution of, for example, Venus, Io or the Archaean Earth. For example, our results show that the plutonic squishy lid regime is characterized by high surface heat flux, which is thought to be the case in the Archaean Earth[41]. If this is the case, and a plutonic squishy lid operated in the early Earth, then we can expect fast cooling of the Earth, which has implications for the time of initiation of plate tectonics: plate tectonics needs a lithosphere thick, cold and dense enough to initiate subduction and keep it self-sustaining[42].

The main lessons of this study can be summarized as follows: intrusive magmatism and a strong partitioning of HPEs both thin the lithosphere, leading to the recycling of basalt into the mantle and an efficient mantle cooling. Furthermore, a depleted mantle allows the formation of little melt and therefore tends to warm up, whereas a re-fertilized mantle can continuously melt and keep cooling down efficiently.

Our results also emphasize the fundamental importance of melting, crust production, the recycling of compositional heterogeneities in the mantle and the partitioning of HPEs into the melt phase. Purely thermal studies, which neglect these compositional effects, can lead to unrealistic results and non-events such as the Earth's Archaean thermal catastrophe[43]. We demonstrate here that crustal recycling, controlled by the mode of magmatism and the partitioning of HPEs, is a process as important as what boundary layer theory based on pure thermal convection has been dictating over the last decades. Crustal recycling could be relatively simple to take into account in zero-dimensional parameterized studies of planet evolution[15], by increasing the diffusive heat flow and not assuming that all of the erupted basalt can be stored in the lithosphere. The present work could be used in such studies to calibrate surface heat flows and internal depletion. Our work has further implications for the surface conditions, outgassing and atmospheric evolution of rocky bodies such as extra-solar terrestrial planets, for which there is an active debate about their interior and tectonic states[44–48]. Outgassing and volatile recycling are strongly affected by the intrusive/extrusive balance. Higher gravity causes a rapid increase of pressure with depth, suppressing decompression melting, thus leading to a higher mantle temperature. Crustal thicknesses should also decrease due to the shallower depth of eclogitization, which may result in an increase in eruption efficiency due to the absence of a thick low-viscosity lower crust[39]. As a result of these, the active tectonic regimes, crustal recycling, degassing and conditions for the onset of plate tectonics on super-Earths[44–46] may notably differ from those on Earth, requiring further investigation along the lines presented here.

Methods

Methods, including statements of data availability and any associated accession codes and references, are available at https://doi.org/10.1038/s41561-018-0094-8.

Received: 2 November 2017; Accepted: 2 March 2018;
Published online: 9 April 2018

References

1. Schubert, G., Turcotte, D. L. & Olson, P. *Mantle Convection in the Earth and Planets* (Cambridge Univ. Press, Cambridge, 2001).
2. Turcotte, D. L. & Schubert, G. *Geodynamics* (Cambridge Univ. Press, Cambridge, 2014).
3. Ruiz, J. et al. The thermal evolution of Mars as constrained by paleo-heat flows. *Icarus* **215**, 508–517 (2011).
4. Warren, P. H. & Rasmussen, K. L. Megaregolith insulation, internal temperatures, and bulk uranium content of the moon. *J. Geophys. Res. Solid Earth* **92**, 3453–3465 (1987).
5. Veeder, G. J., Matson, D. L., Johnson, T. V., Davies, A. G. & Blaney, D. L. The polar contribution to the heat flow of Io. *Icarus* **169**, 264–270 (2004).
6. Peale, S. J., Cassen, P. & Reynolds, R. T. Melting of Io by tidal dissipation. *Science* **203**, 892–894 (1979).
7. O'Reilly, T. C. & Davies, G. F. Magma transport of heat on Io: a mechanism allowing a thick lithosphere. *Geophys. Res. Lett.* **8**, 313–316 (1981).
8. Breuer, D. & Moore, W. B. in *Treatise on Geophysics* (ed. Schubert, G.) 299–348 (Elsevier, Oxford, 2007).
9. Moore, W. B. & Webb, A. A. G. Heat-pipe Earth. *Nature* **501**, 501–505 (2013).
10. Gerya, T. *Introduction to Numerical Geodynamic Modelling* (Cambridge Univ. Press, Cambridge, 2010).
11. Hofmann, A. W. Mantle geochemistry: the message from oceanic volcanism. *Nature* **385**, 219–229 (1997).
12. Ogawa, M. Effects of chemical fractionation of heat-producing elements on mantle evolution inferred from a numerical-model of coupled magmatism mantle convection system. *Phys. Earth Planet. Inter.* **83**, 101–127 (1994).
13. Xie, S. & Tackley, P. J. Evolution of U-Pb and Sm-Nd systems in numerical models of mantle convection and plate tectonics. *J. Geophys. Res. Planets* **109**, B11204 (2004).

14. Nakagawa, T. & Tackley, P. J. Deep mantle heat flow and thermal evolution of the Earth's core in thermochemical multiphase models of mantle convection. *Geochem. Geophys. Geosyst.* **6**, Q08003 (2005).
15. Kite, E. S., Manga, M. & Gaidos, E. Geodynamics and rate of volcanism on massive Earth-like planets. *Astrophys. J.* **700**, 1732–1749 (2009).
16. Ogawa, M. A positive feedback between magmatism and mantle upwelling in terrestrial planets: implications for the Moon. *J. Geophys. Res. Planets* **119**, 2317–2330 (2014).
17. Lourenço, D. L., Rozel, A. & Tackley, P. J. Melting-induced crustal production helps plate tectonics on Earth-like planets. *Earth Planet. Sci. Lett.* **439**, 18–28 (2016).
18. Armann, M. & Tackley, P. J. Simulating the thermochemical magmatic and tectonic evolution of Venus's mantle and lithosphere: two-dimensional models. *J. Geophys. Res. Planets* **117**, E12003 (2012).
19. Crisp, J. A. Rates of magma emplacement and volcanic output. *J. Volcanol. Geotherm. Res.* **20**, 177–211 (1984).
20. Cawood, P. A., Hawkesworth, C. J. & Dhuime, B. The continental record and the generation of continental crust. *Bull. Geol. Soc. Am.* **125**, 14–32 (2013).
21. Gerya, T. V. Plume-induced crustal convection: 3D thermomechanical model and implications for the origin of novae and coronae on Venus. *Earth Planet. Sci. Lett.* **391**, 183–192 (2014).
22. Stofan, E. R., Smrekar, S. E., Tapper, S. W., Guest, J. E. & Grindrod, P. M. Preliminary analysis of an expanded corona database for Venus. *Geophys. Res. Lett.* **28**, 4267–4270 (2001).
23. Glaze, L. S., Stofan, E. R., Smrekar, S. E. & Baloga, S. M. Insights into corona formation through statistical analyses. *J. Geophys. Res. Planets* **107**, 18–12 (2002).
24. Krassilnikov, A. S. & Head, J. W. Novae on Venus: geology, classification, and evolution. *J. Geophys. Res. Planets* **108**, 5108 (2003).
25. Rozel, A. B., Golabek, G. J., Jain, C., Tackley, P. J. & Gerya, T. Continental crust formation on early Earth controlled by intrusive magmatism. *Nature* **545**, 332–335 (2017).
26. Tackley, P. J. Modelling compressible mantle convection with large viscosity contrasts in a three-dimensional spherical shell using the yin-yang grid. *Phys. Earth Planet. Inter.* **171**, 7–18 (2008).
27. Hernlund, J. W. & Tackley, P. J. Modeling mantle convection in the spherical annulus. *Phys. Earth Planet. Inter.* **171**, 48–54 (2008).
28. Kaufmann, G. & Lambeck, K. Mantle dynamics, postglacial rebound and the radial viscosity profile. *Phys. Earth Planet. Inter.* **121**, 301–324 (2000).
29. Mitrovica, J. X. & Forte, A. M. A new inference of mantle viscosity based upon joint inversion of convection and glacial isostatic adjustment data. *Earth Planet. Sci. Lett.* **225**, 177–189 (2004).
30. Sleep, N. H. Segregation of magma from a mostly crystalline Mush. *Bull. Geol. Soc. Am.* **85**, 1225–1232 (1974).
31. McKenzie, D. The generation and compaction of partially molten rock. *J. Petrol.* **25**, 713–765 (1984).
32. Fowler, A. C. A mathematical model of magma transport in the asthenosphere. *Geophys. Astrophys. Fluid Dyn.* **33**, 63–96 (1985).
33. Scott, D. R. & Stevenson, D. J. Magma ascent by porous flow. *J. Geophys. Res. Solid Earth* **91**, 9283–9296 (1986).
34. Bercovici, D., Ricard, Y. & Schubert, G. A two-phase model for compaction and damage: 1. general theory. *J. Geophys. Res. Solid Earth* **106**, 8887–8906 (2001).
35. Keller, T., May, D. A. & Kaus, B. J. P. Numerical modelling of magma dynamics coupled to tectonic deformation of lithosphere and crust. *Geophys. J. Int.* **195**, 1406–1442 (2013).
36. O'Neill, C., Moresi, L. & Lenardic, A. Insulation and depletion due to thickened crust: effects on melt production on Mars and Earth. *Geophys. Res. Lett.* **32**, L14304 (2005).
37. Cooper, C. M., Lenardic, A. & Moresi, L. Effects of continental insulation and the partitioning of heat producing elements on the Earth's heat loss. *Geophys. Res. Lett.* **33**, 4741 (2006).
38. Deschamps, F., Cobden, L. & Tackley, P. J. The primitive nature of large low shear-wave velocity provinces. *Earth Planet. Sci. Lett.* **349**, 198–208 (2012).
39. Gerya, T. V. & Burg, J.-P. Intrusion of ultramafic magmatic bodies into the continental crust: Numerical simulation. *Phys. Earth Planet. Inter.* **160**, 124–142 (2007).
40. Wood, B. J. & Blundy, J. D. in *Treatise on Geochemistry* (eds Holland, H. D. & Turekian, K. K.) 395–424 (Elsevier, Oxford, 2003).
41. Lenardic, A. in *Archean Geodynamics and Environments* Vol. 164 (eds Benn, K. et al.) 33–45 (American Geophysical Union, 2006).
42. van Hunen, J. & van den Berg, A. P. Plate tectonics on the early Earth: limitations imposed by strength and buoyancy of subducted lithosphere. *Lithos* **103**, 217–235 (2008).
43. Christensen, U. R. Thermal evolution models for the Earth. *J. Geophys. Res. Solid Earth* **90**, 2995–3007 (1985).
44. Valencia, D., O'Connell, R. J. & Sasselov, D. D. Inevitability of plate tectonics on super-Earths. *Astrophys. J.* **670**, L45–L48 (2007).
45. Stein, C., Finnenkötter, A., Lowman, J. P. & Hansen, U. The pressure-weakening effect in super-Earths: consequences of a decrease in lower mantle viscosity on surface dynamics. *Geophys. Res. Lett.* **38**, L21201 (2011).
46. van Heck, H. J. & Tackley, P. J. Plate tectonics on super-Earths: equally or more likely than on Earth. *Earth Planet. Sci. Lett.* **310**, 252–261 (2011).
47. Tackley, P. J., Ammann, M., Brodholt, J. P., Dobson, D. P. & Valencia, D. Mantle dynamics in super-Earths: post-perovskite rheology and self-regulation of viscosity. *Icarus* **225**, 50–61 (2013).
48. Dorn, C. et al. Can we constrain the interior structure of rocky exoplanets from mass and radius measurements? *Astron. Astrophys.* **577**, A83 (2015).

Acknowledgements

We thank A. Püsök, G. Golabek and S. Labrosse for reading an earlier version of the manuscript. D.L.L. was supported by ETH Zurich grant ETH-46 12-1. A.B.R. and P.J.T. received funding from the European Research Council under the European Union's Seventh Framework Programme (FP/2007-2013)/ERC Grant Agreement no. 320639 project iGEO. T.G. received funding from the European Union's Horizon 2020 research and innovation programme under the Marie Sklodowska-Curie grant agreements no. 642029-ITN CREEP and no. 674899 SUBITOP.

Author contributions

D.L.L., A.B.R and T.G. designed the set of numerical simulations. P.J.T. implemented the eruption–intrusion routines on the convection code and initiated this general research direction. D.L.L. wrote the post-processing routines. D.L.L. and A.B.R. produced the figures. All authors contributed to the manuscript.

Competing interests

The authors declare no competing interests.

Additional information

Supplementary information is available for this paper at https://doi.org/10.1038/s41561-018-0094-8.

Reprints and permissions information is available at www.nature.com/reprints.

Correspondence and requests for materials should be addressed to D.L.L.

Publisher's note: Springer Nature remains neutral with regard to jurisdictional claims in published maps and institutional affiliations.

Methods

Numerical modelling of thermochemical convection. Here, we perform simulations of thermochemical compressible mantle convection using the code StagYY[26] in a two-dimensional spherical annulus[27]. StagYY uses a finite-volume discretization of the governing compressible anelastic equations for conservation of mass, momentum and energy[1]. Tracers are used to track composition and heat-producing elements (HPEs), and to allow for the treatment of partial melting and crustal formation. A direct solver is employed to obtain a solution of the Stokes and continuity equations, using the PETSc toolkit[49]. The heat equation is solved in two steps: advection is performed using the MPDATA scheme and diffusion is then solved implicitly using a PETSc solver. Free-slip boundary conditions are employed at the surface and core–mantle boundary to address the thermochemical evolution of an Earth-like planet over 4.5 billion years. The temperature at the surface is fixed to 300 K. Core cooling is assumed[50–52]. The domain is decomposed into 512 (laterally) by 64 (radially) cells, in which around one million tracers are advected.

A parameterization based on mineral physics data[53,54] is included in the model, dividing minerals into the olivine and pyroxene–garnet systems, which undergo different solid–solid phase transitions, as used in previous studies[13,55]. The mixture of minerals depends on the chemical composition, which varies between two endmembers: basalt (pure pyroxene–garnet) and harzburgite (75% olivine). As in previous studies[13,17,55], changes in composition arise from melt-induced differentiation. At each time step, the temperature in each cell is compared to the solidus temperature, which is a function that fits experimental data for the upper[56] and the lower mantle[57]. If the temperature in a specific cell exceeds the solidus, then enough melt is generated to bring the temperature back to solidus, leaving a more depleted residue behind depending on the degree of melt generated. Melting can occur only if the material is not completely depleted. The solidus temperature increases by 60 K with depletion, from pyrolite to harzburgite. The generated melt is then emplaced in the form of extrusive volcanics or intrusive plutons, in a predefined proportion. This proportion is kept constant throughout each simulation, and can be written as:

$$\mathrm{EE}(\%) = 100 - \mathrm{IE}(\%)$$

where EE is the extrusion efficiency and IE is the intrusion efficiency. It is assumed that the percolation of melt through the solid is much faster than convection[58]. Thus, part of the shallow melt is instantly removed and extruded to the surface to form oceanic crust with the surface temperature, while the rest is intruded at the base of the crust[59]. An important difference between these two modes is that the extruded magma loses the heat it carries to the atmosphere, while the intruded one carries its heat to the place where it is emplaced.

The density is computed as the sum of pressure, thermal and compositional effects. Pressure is taken into account using a third-order Birch–Murnaghan equation of state[47]. Diffusion creep, with the assumption of homogeneous grain size, is the assumed viscous deformation mechanism. It follows a temperature- and pressure-dependent Arrhenius law:

$$\eta_{diff}(T,p) = \eta_0 \exp\left(\frac{E - pV}{RT} - \frac{E}{RT_0}\right)$$

where η_0 is the reference viscosity at zero pressure and reference temperature T_0 (equal to 1,600 K), E is the activation energy, p is the pressure, V is the activation volume, T is the absolute temperature and R is the gas constant. Different values for E and V are used for the upper and lower mantle[60,61]. Three sets of simulations are presented in this work, portraying three different reference viscosity values, 10^{20}, 3×10^{20} and 10^{21} Pa s. It is assumed that the material deforms plastically after reaching a yield stress, σ_y, defined as:

$$\sigma_y = \sigma_{duct} + \sigma'_{duct} p$$

where σ_{duct} is the surface ductile yield stress and σ'_{duct} is the vertical gradient of the ductile yield stress. In practice, this last parameter prevents yielding in the deep mantle. The parameter with the greatest influence in the previous equation is σ_{duct}. In the present simulations, it is set to a very high value 300 MPa, to avoid yielding (subduction). The effective viscosity, combining diffusion creep and plastic yielding, is given by:

$$\eta_{eff} = \left(\frac{1}{\eta_{diff}} + \frac{2\mathring{\varepsilon}}{\sigma_y}\right)^{-1}$$

where $\mathring{\varepsilon}$ is the second invariant of the strain rate tensor. The viscosity is not directly dependent on melt fraction or composition. A viscosity jump factor of 10 is imposed at the transition between the upper and lower mantle[62]. A second viscosity jump factor of 10^{-3} (compared with the above material) is imposed at the transition to post-perovskite at the lowermost mantle depths, as suggested by mineral physics experiments and theoretical calculations[63].

The initial potential temperature in the simulations presented in this work is 1,917 K, an adequate initial state on the Earth's evolution starting from the Precambrian[64]. Due to the higher temperature in the planet's mantle and due to intrusion, pockets of high melt fraction are expected. Largely molten silicates have very low viscosities, on the order of $\eta_{liq\text{-}sil} \approx 0.1 - 100$ Pa s (ref. [65]). Due to the low viscosity, the Rayleigh number is expected to be very high, leading to very efficient cooling. To simulate this fast cooling in the modelled (geological) timescales, an effective thermal conductivity method is employed for high fractions of magma. We parameterize the heat flux, J_q, as done in other studies[65]:

$$J_q = -k_h\left[\frac{\partial T}{\partial r} - \left(\frac{\partial T}{\partial r}\right)_s\right] - k\frac{\partial T}{\partial r}$$

where k is the thermal conductivity, k_h is the effective thermal conductivity, $(\partial T/\partial r)_s$ is the adiabatic temperature gradient and r is the radius. k_h is a function of the melt fraction, and its value is 10^5 W (mK)$^{-1}$ for melt fractions higher than 60%, negligible (~0) when melt fractions are lower than 20%, and a hyperbolic tangent step function in-between the values of ~0 and 10^5 W (mK)$^{-1}$ for melt fractions in-between 20% and 60%. This smooth step function reflects the fact that when the melt fraction in a partially molten rock is higher than a certain critical value, generally taken as around 40%, solid particles are disconnected and the viscosity is controlled by that of the melt[65–67]. In practice, k_h implies that low-viscosity high-melt-fraction molten rocks transport heat five orders of magnitude faster than solid rock, as the maximum value of k_h is 10^5 W (mK)$^{-1}$, and k, the thermal conductivity of a lithospheric solid rock, is typically a value of around 3 W (mK)$^{-1}$.

For more information about the model and values used for the standard physical parameters, see ref. [17], and references therein, on which the model used in this study is based. For more details on the code StagYY, see ref. [26].

Code availability. The convection code StagYY is the property of P.J.T. and Eidgenössische Technische Hochschule Zürich (ETH), and is available for collaborative studies from P.J.T. (paul.tackley@erdw.ethz.ch).

Data availability. The data that support the findings of this study are available from the corresponding author upon reasonable request.

References

49. Balay, S., Brown, J., Buschelman, K. & Eijkhout, V. *PETSc Users Manual* Revision 3.3 (Argonne National Laboratory, 2012).
50. Buffett, B. A., Huppert, H. E., Lister, J. R. & Woods, A. W. Analytical model for solidification of the Earth's core. *Nature* **356**, 329–331 (1992).
51. Buffett, B. A., Huppert, H. E., Lister, J. R. & Woods, A. W. On the thermal evolution of the Earth's core. *J. Geophys. Res. Solid Earth* **101**, 7989–8006 (1996).
52. Nakagawa, T. & Tackley, P. J. Effects of thermo-chemical mantle convection on the thermal evolution of the Earth's core. *Earth Planet. Sci. Lett.* **220**, 107–119 (2004).
53. Irifune, T. & Ringwood, A. E. Phase transformations in subducted oceanic crust and buoyancy relationships at depths of 600–800 km in the mantle. *Earth Planet. Sci. Lett.* **117**, 101–110 (1993).
54. Ono, S., Ito, E. & Katsura, T. Mineralogy of subducted basaltic crust (MORB) from 25 to 37 GPa, and chemical heterogeneity of the lower mantle. *Earth Planet. Sci. Lett.* **190**, 57–63 (2001).
55. Nakagawa, T. & Tackley, P. J. Influence of magmatism on mantle cooling, surface heat flow and Urey ratio. *Earth Planet. Sci. Lett.* **329-330**, 1–10 (2012).
56. Herzberg, C., Raterron, P. & Zhang, J. New experimental observations on the anhydrous solidus for peridotite KLB-1. Geochem. Geophys. Geosyst. https://doi.org/10.1029/2000GC000089 (2000).
57. Zerr, A., Diegeler, A. & Boehler, R. Solidus of Earth's deep mantle. *Science* **281**, 243–246 (1998).
58. Condomines, M., Hemond, C. & Allegre, C. J. U-Th-Ra radioactive disequilibria and magmatic processes. *Earth Planet. Sci. Lett.* **90**, 243–262 (1988).
59. Vogt, K., Gerya, T. V. & Castro, A. Crustal growth at active continental margins: numerical modeling. *Phys. Earth Planet. Inter.* **192-193**, 1–20 (2012).
60. Karato, S. I. & Wu, P. Rheology of the upper mantle: a synthesis. *Science* **260**, 771–778 (1993).
61. Yamazaki, D. & Karato, S.-I. Some mineral physics constraints on the rheology and geothermal structure of Earth's lower mantle. *Am. Mineral.* **86**, 385–391 (2001).
62. Čížková, H., van den Berg, A. P., Spakman, W. & Matyska, C. The viscosity of Earth's lower mantle inferred from sinking speed of subducted lithosphere. *Phys. Earth Planet. Inter.* **200–201**, 56–62 (2012).
63. Ammann, M. W., Brodholt, J. P., Wookey, J. & Dobson, D. P. First-principles constraints on diffusion in lower-mantle minerals and a weak D″ layer. *Nature* **465**, 462–465 (2010).
64. Herzberg, C., Condie, K. & Korenaga, J. Thermal history of the Earth and its petrological expression. *Earth Planet. Sci. Lett.* **292**, 79–88 (2010).
65. Abe, Y. in *Evolution of the Earth and Planets* Vol. 74 (eds Takahashi, E. et al.) 41–54 (American Geophysical Union, 1993).
66. Arzi, A. A. Critical phenomena in the rheology of partially melted rocks. *Tectonophysics* **44**, 173–184 (1978).
67. Costa, A., Caricchi, L. & Bagdassarov, N. A model for the rheology of particle-bearing suspensions and partially molten rocks. *Geochem. Geophys. Geosyst.* **10**, Q03010 (2009).